The *PPE25 (Rv1787)- PE18 (Rv1788)- PPE26 (Rv1789)* gene cluster is involved in immune evasion by *Mycobacterium tuberculosis*

Ravi Prasad Mukku[1], Kokavalla Poornima[1], Korak Chakraborty[1,2] and Tirumalai R. Raghunand[1,2*]

[1]CSIR - Centre for Cellular and Molecular Biology, Uppal Road, Hyderabad 500007, India

[2]Academy of Scientific and Innovative Research (AcSIR), Ghaziabad 201002, India

Email information:

Ravi Prasad Mukku - raviprasad.mukku@ccmb.res.in

Kokavalla Poornima - poornima.kchowdary@gmail.com

Korak Chakraborty - korak.chakraborty@ccmb.res.in

Tirumalai R. Raghunand - raghu@ccmb.res.in. *Correspondence and reprints

Keywords: *Mycobacterium tuberculosis*; PE_PPE family; Macrophages; TLR2; Immunomodulation

ABSTRACT

Mycobacterium tuberculosis (M. tb) the causative agent of human tuberculosis, is one of the most successful pathogens known to man. The key to its success is the multiple factors it encodes to subvert host immune responses. One such class of virulence factors is encoded by the multigenic PE_PPE family which accounts for 10% of the coding potential of the *M. tb* genome, and is primarily found in pathogenic mycobacteria. A number of these genes occur in clusters, of which the *PPE25 (Rv1787)-PE18 (Rv1788)-PPE26 (Rv1789)* locus is the only one organised in a *PPE-PE-PPE* arrangement. We establish here that this cluster is co-operonic in *M. tb*, and in a pairwise interaction screen, identify PPE25::PPE26 as the only interacting protein pair encoded by this cluster. In the THP-1 macrophage infection model, recombinant *M. smegmatis* strains expressing *PPE25*, *PE18*, and *PPE26*, exhibited enhanced survival compared to the control. Consistent with this finding, was the decrease in inducible nitric oxide synthase (*iNOS2*) transcript levels in these macrophages. We also observed a significant increase in levels of the anti-inflammatory cytokine *IL-10*, and a reduction in levels of the pro-inflammatory cytokine *IL-12* upon infection. Macrophages infected with recombinant *M. smegmatis* expressing *PPE26* showed increased phosphorylation of the MAP kinase p38, consistent with the known TLR2 binding activity of PPE26. In contrast to strains expressing the individual cluster genes, the recombinant *M. smegmatis* strain expressing the entire *PPE25-PE18-PPE26* operon showed no change in intra-macrophage CFUs in comparison to the control strain, which is suggestive of an inhibitory role for the PPE25-PPE26 complex in CFU enhancement. Taken together, our findings implicate the *PPE25-PE18-PPE26* cluster in playing an immune evasion role in the pathophysiology of *M. tb*.

INTRODUCTION

Despite the best efforts of macrophages to eradicate intracellular bacteria through various antimicrobial processes, *M. tb* possesses the ability to thrive and persist within these cells by altering their immediate antimicrobial actions and evading the host immune system (1-3). Mycobacteria have highly hydrophobic and impenetrable cell walls, and therefore need very specific and efficient mechanisms to secrete the effectors needed for their immune evasion function. Mycobacteria encode an atypical type VII secretion apparatus, commonly known as the ESX system, and also contain transporters known in other bacteria (4, 5). A growing body of evidence has revealed that the multigenic PE/PPE proteins are either secreted from or associated with the mycobacterial cell envelope, and play a key role in mediating host-pathogen interactions (6-10). Recent reports suggest that these proteins are linked to antigenic diversity, host-pathogen interactions, and immune evasion(1-3, 7, 10), but our understanding of the molecular basis of their functioning remains limited.

Interestingly, the 12 gene ESX-5 locus contains two clusters of members of the PE_PPE family of proteins, including a three gene segment encoding PPE25 (*Rv1787*), PE18 *(Rv1788)*, and PPE26 (*Rv1789*) (4, 11). The *M. tb* Δ*PPE25-PE19* mutant containing a deletion in 5 PE_PPE genes encoded in the *esx5* locus was shown to be avirulent in immunocompetent mice. This strain however remained strongly immunogenic and showed a greater protective efficacy against *M. tb* infection than BCG (12). This 5 gene deletion strain also showed reduced virulence in murine macrophages, and in a SCID mouse model of *M. tb* infection (11). Several bacterial processes, including replication, vacuole acidification, and phagolysosome fusion in macrophages, were affected when the gene homologous to *PPE25* was deleted from *Mycobacterium avium* (13). PPE25 has been used as a strong T-cell epitope for a DNA vaccine against *M. tb* (14). Moreover, the expression of the *PPE25*, *PE18* and *PPE26* transcripts were observed to be upregulated under conditions of hypoxia/ dormancy, and NO stress (15, 16). Taken together, these observations are strongly suggestive of a significant role for this segment in the pathophysiology of *M. tb,* warranting an investigation into the functions of these genes. Hence, we chose to functionally evaluate this cluster, to gain an enhanced understanding of its role in *M. tb* pathogenesis.

MATERIALS AND METHODS

Bacterial strains, media and growth conditions

M. smegmatis mc^{2}6 and *M. tb* H37Rv were cultivated in Middlebrook, 7H9 broth and 7H10 agar (Difco) containing albumin dextrose complex (5 g BSA, 2 g glucose, and 0.85 g NaCl/L), 0.5% (v/v) glycerol, and 0.5% (v/v) Tween 80. Luria Bertani medium was used to cultivate *E. coli* strains - both *E. coli* and mycobacteria were cultured by shaking at 37° C. When required, 200 µg/ml of ampicillin and 50 µg/ml of kanamycin (for *E. coli*) and 15 µg/ml of kanamycin (for mycobacteria) were added to the culture medium.

DNA techniques

All restriction enzymes, T4 DNA ligase, and Taq polymerase were purchased from New England Biolabs (NEB) and Invitrogen, respectively. DNA manipulation protocols including plasmid DNA preparation, restriction endonuclease digestion, agarose gel electrophoresis, ligation of DNA fragments and *E. coli* transformation were performed according to (17). The PCR amplifications were performed according to the manufacturer's instructions. During each cycle, 95° C was held for 30 s, 60° C for 30 s, and 72° C for 1 min, followed by a 72° C extension cycle for 10 min. The Qiagen gel extraction kit was used to purify DNA fragments for cloning reactions according to the manufacturer's instructions. *M. smegmatis* was transformed by electroporation.

In silico analyses

All *M. tb* sequences were obtained from the Mycobrowser database (https://mycobrowser.epfl.ch/). The TM-pred (18) and Kyte& Doolittle (19) algorithms were used to identify trans-membrane domains and regions of hydrophobicity respectively.

Sub-cellular localisation and Proteinase K sensitivity assay

In order to determine the subcellular location of these proteins, the *M. tb PPE25*, *PE18, PPE26* ORFs were cloned between *BamHI* and *EcoRI* sites of pJEX55 (20) and the recombinant plasmids were transformed into *M. smegmatis*. The recombinant *M. smegmatis* strains expressing c-myc tagged PPE25, PE18, PPE26 were harvested at the logarithmic phase of growth, washed and resuspended in

PBS. The samples were divided into two identical aliquots and incubated at 37°C for 30 min with or without Proteinase K (Sigma). With the addition of 2 mM EGTA, the reaction was stopped, and the sub-cellular fractions of these samples were isolated as described in (21). The individual fractions were separated using denaturing SDS PAGE, and the fusion proteins were detected by western blotting with anti-c-myc antibodies (sc40, Santa Cruz).

Expression of PPE25, PE18, and PPE26 in *M. smegmatis*

M. tb PPE25, PE18, PPE26 ORFs were amplified using gene-specific primers (Table S1) and cloned between the *BamHI* and *EcoRI* sites of pMV261(22). These constructs were then transformed into *M. smegmatis* for overexpression.

Expression and purification of PPE25 and PPE26

The full-length *M. tb PPE25* and *PPE26* ORFs were cloned as C-terminal 6xHis-tagged fusion in pET22b, and N-terminal Glutathione-S-Transferase (GST) tagged fusion in pGEX6p1 respectively. Following sequence confirmation, the constructs were transformed into *E. coli* BL21(DE3). For induction, cultures were allowed to grow to an OD of 0.5, and induced with 0.5 mM IPTG. His-tagged PPE25 was purified using Ni-NTA affinity chromatography and GST tagged PPE26 was purified using glutathione agarose beads. The purified proteins were used for pull-down experiments.

***In vitro* growth kinetics**

To functionally characterise *M. tb PPE25, PE18,* PPE26, their ORFs were amplified from *M. tb* H37Rv genomic DNA using gene specific primers (Table S1), cloned between the *BamHI* and *EcoRI* sites of pMV261 (23) and transformed into *M.smegmatis*. To examine their growth patterns, recombinant *M. smegmatis* strains were grown until late exponential phase, diluted to an OD of 0.2, and cultured in Middlebrook 7H9 broth containing 15 µg/ml kanamycin. Growth curves were generated by CFU measurements and plotted against time. At each designated time point, cultures were harvested for RNA extraction and gene expression analyses performed. All CFU enumeration assays were performed in the presence of 15 µg/ml kanamycin.

Macrophage infection

THP-1 monocytes were cultured at 37° C in 5% CO_2 in RPMI 1640 medium supplemented with 10% (v/v) Fetal bovine serum and antibiotics (60 µg/ml penicillin G sodium, 50 µg/ml streptomycin sulphate, and 30 µg/ml gentamycin sulphate). For the infection experiments, monocytes were seeded at a density of $2x10^6$/well for 24 h, differentiated with 5 ng/ml PMA, and then infected 72 h later. Cultures of exponentially growing bacteria were pelleted, washed, resuspended in RPMI medium (without antibiotics) to an OD of 1.0. Single cell suspensions of recombinant *M. smegmatis* strains were prepared by passing culture suspensions 5-6 times through a 26 1/2 gauge needle. At each step, CFU counts were performed to determine bacterial viability. Based on pilot infections with multiple MOIs, equal numbers of each strain were used for infections (Input counts) at a MOI of 1:100. Post-infection CFU counts were determined by lysis of infected cells after 2 h of incubation with bacteria (T_0 counts). In order to kill extracellular bacteria, complete RPMI containing gentamycin was added. To determine CFU counts, infected cells were lysed with 0.1% Triton X-100 and plated on Middlebrook 7H10 agar at the designated time points. For each experiment, macrophages infected with *M. smegmatis* expressing the empty vector were used as controls.

Real-time RT-PCR analysis

The expression profiles of *PPE25*, *PE18 PPE26* in *M. tb* and in recombinant strains of *M. smegmatis* expressing pMV261-*PPE25*, pMV261-*PE18* pMV261-*PPE26* as a function of growth, were determined using real-time transcript measurements. For this, cells were harvested at OD 0.8, 1.5, 2, 3, 3.5, and at 4, 8, 12, 24, 48 and 72 h time points respectively, and total RNA was isolated from each culture using TRIzol reagent (Invitrogen) as per the manufacturer's protocol. Following treatment with RNAse free DNAse I, cDNA synthesis was performed using the iScript cDNA synthesis kit (Bio-Rad) and subsequently used as a template for SYBR green based PCR amplification using *PPE25*, *PE18, PPE26* specific primers (Table S1) to generate 200 bp amplicons. Gene specific transcript levels in *M. smegmatis* were normalised to the *sigA* transcript in each sample, and in *M. tb* to the 16s rRNA transcript. In *M. smegmatis* the relative fold change in transcript levels at each time point was calculated with respect to the levels at 4 h. In the *M. tb* expression profile,

the relative fold change in transcript at each OD point was calculated with respect to the levels at OD 0.8. To quantify host cytokines and *iNOS2* transcript levels, total RNA was isolated from infected macrophages using TRIzol reagent. Following treatment with RNAse free DNAse I, cDNA synthesis was performed using the iScript cDNA synthesis kit (Bio-Rad) and subsequently used as a template for SYBR green based PCR amplification using primers specific to *iNOS2*, *IL-10*, *IL-12* (Table S1) designed to generate 200 bp amplicons. The levels of each mRNA were normalised to the transcript levels of GAPDH and β-actin. Relative fold change was calculated with reference to macrophages infected with *M. smegmatis* expressing the empty vector.

Western blotting

The levels of total and phosphorylated P38 in infected THP-1 macrophages were determined by western blot analysis. Each sample was lysed in RIPA lysis buffer, following which, equal protein amounts from each cell lysate subjected to SDS-PAGE and transferred onto PVDF membranes. Each blot was sequentially probed with antibodies specific to phosphorylated or total p38 (Cell Signalling Technology) and β-actin. Proteins were detected using Enhanced Chemiluminescence (Santa Cruz). Recombinant *M. smegmatis* containing pMV261 was used as an empty vector/ mock control. For quantitation, the intensity of all bands was densitometrically measured using ImageJ and normalised to levels of β-actin. The normalised levels of phosphorylated p38 in control samples (pMV261) were assigned a value of 1, and the fold change in the levels of these proteins in the test samples (PPE25, PE18, PPE26) were derived with respect to the control.

Co-transcriptional analysis

Total RNA extracted from exponentially growing *M. tb* H37Rv was used to assess the transcriptional state of the *PPE25-PE18-PPE26* cluster. RNA treated with DNAse I was used as a template for cDNA synthesis with the primers *PPE26* R1 (Table S1). The cDNA was utilised for PCR amplification with gene-specific primer combinations. The analysis includes the appropriate negative controls (-RT).

Co-immunoprecipitation

To perform *in vivo* pull down assays, 150 ml of independent *M. smegmatis* cultures co-transformed with pJEX55+pSCW54, pJEX55-*PPE26*+pSCW54, pJEX55+pSCW54-*PPE25,* pJEX55-*PPE26*+pSCW54-*PPE25* were grown in Middlebrook 7H9 broth containing kanamycin and hygromycin to log phase and induced with 0.2% acetamide for 6 h. Induced cells were pelleted, resuspended in 1.2 ml PBS containing protease inhibitors and lysed by sonication. Half of this lysate was used to prepare a cell envelope fraction by ultracentrifugation (21) and the pellets were resuspended in 150 µl of PBS containing protease inhibitors and 0.5% CHAPS. 400 µl of cell lysates were mixed with 50 µl of the solubilised cell envelope fraction and the protein amounts in the mix were quantitated using a Bradford assay. For the co-IP assay 500 µg of protein in a total volume of 500 µl PBS, was incubated with an anti c-myc antibody; prior to antibody addition, 30 µl of the reaction mix was removed and saved as a loading control. Protein A agarose beads were then added to each sample and incubated at 4°C for 6 h. Following three washes with PBS, the beads were boiled in 50 µl of sample buffer and subjected to SDS-PAGE. Separated proteins were transferred to PVDF and probed with an anti-His antibody.

Mycobacterial Protein Fragment Complementation (MPFC) assay

To assess the interaction of PPE25-PE18, PE18-PPE26 and PPE25-PPE26 *in vivo*, *PPE25, PE18* and *PPE26* were cloned into the *E. coli* - *Mycobacterium* shuttle vectors pUAB400 and pUAB300 respectively. Both constructs were co-transformed in *M. smegmatis* mc^2155 and the interaction assay was performed as described (24). Appropriate positive (pUAB100+pUAB200) and negative (pUAB100+pUAB400, pUAB400+ pUAB300) controls were included in the assay.

RESULTS

PPE25, *PE18* and *PPE26* are co-operonic and the *PPE25* and *PPE26* gene products interact

The *PPE25-PE18-PPE26* cluster, is the only one of 40 clusters of PE/PPE genes in the *M. tb* genome that has a *PE* gene that is directly flanked by two *PPE* genes, in a tandem arrangement (7). Its predicted co-operonic status (25), is based on the short spacing between the genes - 78 base separating *PPE25-PE18*, and 13 bp separating *PE18-PPE26* (Fig. 1A). To confirm this prediction, RT-PCR experiments were carried out with RNA isolated from log phase grown *M. tb* H37Rv using primer

pairs (Table S1) intended to amplify ORF and junction-specific areas of the cluster (Fig. 1A). The sizes of the amplicons obtained (*PPE25*-200 bp, J1-200 bp, *PE18*-200 bp, J2-200bp, *PPE26*-200 bp), and the absence of amplification products in the -RT control lanes, establish that this gene cluster is transcribed as a mono-cistronic message (Fig. 1B).

This observation was further validated by examining the expression levels of the three genes as a function of growth in *M. tb* H37Rv. All the genes were observed to be coordinately expressed (Fig. 1C), confirming the operonic status of this cluster. It is well-known that genes expressed in a single operon have related functions, and their products are most likely to physically interact with each other. To test this possibility, we performed a pairwise screen for interaction between PPE25+PE18, PPE26+PE18, and PPE25+PPE26 using the mycobacterial protein fragment complementation (M-PFC) assay (24). In this screen, the cluster genes were expressed as murine dihydrofolate reductase domain F [1,2] and F [3] fusions, and then co-transformed to *M. smegmatis* mc^2155. Co-transformants for the PPE25-PPE26 pair, were observed to be resistant to 20 µg/ml of trimethoprim (Fig. 1D), demonstrating that PPE25 and PPE26 interact *in vivo*. No growth was observed in the negative control samples and co-transformants for the PPE25+PE18 and PPE26+PE18 pairs, implying that this cluster encodes only one pair of interacting proteins, namely PPE25:PPE26. To confirm this interaction, we performed an *in vivo* pull-down in *M. smegmatis,* which lacks this gene pair. PPE25 and PPE26 were shown to co-precipitate in this experiment (Fig. 1D), proving that the two proteins indeed interact *in vivo*; we ensured equal loading for each sample (Figure. S1). This interaction could not be tested *in-vitro* since PPE25 cloned with a C-terminal 6xHis tag could be expressed but not purified (Fig. S2A). We however were able to partially purify an N-terminal GST tagged PPE26 (Fig. S2B).

Recombinant strains of *M. smegmatis* expressing *PPE25*, *PE18*, *and PPE26*, show a survival advantage in macrophages

To investigate the functions of PPE25, PE18, and PPE26 in mycobacterial pathophysiology, we used *M. smegmatis* as a surrogate model, the genome of which lacks homologues for the vast majority of PE-PPE proteins, including PPE25, PE18, and PPE26. First, recombinant *M. smegmatis* strains expressing c-myc tagged PPE25, PE18, PPE26 were subjected to Proteinase K treatment and sub-cellular

fractionation to determine the subcellular location of each protein. Each fraction's loading was ensured to be equal (Fig. S3 A, B, C) before their spatial distribution was analysed. Western blotting showed that all three proteins were localised to the cell envelope, and their signals were greatly reduced in the cell wall-associated fractions in the Proteinase K treated samples as compared to the untreated ones (Fig. S3 D, E, F). This showed that PPE25, PE18, and PPE26 were exposed to the cell surface, allowing the use of this model to evaluate their function as modulators of pathogenicity *via* their interactions with the host. Their cell-envelope localisation was consistent with the computationally predicted presence of transmembrane and hydrophobic stretches in these proteins (Fig. S4A, B). Next, we investigated the possible functions of the proteins in modulating host-pathogen interactions using constitutively expressed untagged PPE25, PE18, and PPE26 in *M. smegmatis*. Over-expression of these genes did not cause growth abnormalities *in vitro*, as shown by growth profiling of *M. smegmatis* strains expressing *PPE25*, *PE18*, *PPE26*, the entire operon (*PPE25-PE18-PPE26*), and the empty vector (Fig. S5A, B). Real-time RT-PCR analysis of recombinant *M. smegmatis* strains using gene-specific primers (Table S1) revealed that transcript levels for the three genes were similar, indicating that their expression did not change with growth (Figure S5C, D, E, F). When we infected THP-1 macrophages with these recombinant strains, we observed that the strains expressing *PPE25*, *PPE18*, and *PPE26*, showed a survival advantage over the empty vector containing control strain (Fig. 2A). This elevation in CFU counts, was consistent with the reduction in transcript levels of *iNOS2*, which is primarily responsible for control of bacillary load in this model (Fig. 2C). In contrast to this, the strain expressing the full operon, did not show a change in CFU counts compared to the empty vector control (Fig. 2A). However, while we expected the levels of *iNOS2* to not change in these cells, we observed this transcript to be upregulated compared to the control (Figure. 2C).

***PPE25, PE18,* and *PPE26* modulate the macrophage innate immune response**

The levels of numerous cytokines involved in the control of *M. tb* infection (26), were assessed to evaluate the immunomodulatory potential of PPE25, PE18, and PPE26. Among the anti-inflammatory and pro-inflammatory cytokines we measured, IL-10 and IL-12 showed changes in their expression patterns in THP-1 macrophages infected with the recombinant *M. smegmatis* strains. Macrophages infected with

recombinants expressing *PPE25*, *PPE26*, and the entire operon, showed a significant upregulation in transcript levels of the anti-inflammatory cytokine IL-10, but the same was not observed in cells infected with the *PE18* expressing strain (Fig. 3A). Also, the transcript levels of IL-12, a critical pro-inflammatory cytokine, was seen to be significantly down-regulated in macrophages infected with all the recombinant strains (Fig. 3B). These observations immediately raised the question of the identity of a possible receptor engagement of these proteins, that might induce the changes in cytokine profiles. Since the interaction of PPE26 with macrophage TLR2 had been described (27), we proceeded to verify if signalling through this receptor was being activated in our infection scenario. This was performed by assessing the phosphorylation status of p38, a marker for TLR2 activation, in the lysates of THP-1 macrophages infected with recombinant *M. smegmatis* expressing *PPE25*, *PPE18*, *PPE26*, and the entire operon. An induction in p38 phosphorylation was observed in macrophages infected with *M. smegmatis* recombinants expressing PPE26, and the entire operon, but not in cells infected with recombinants expressing *PPE18* or *PPE25* alone (Fig. 4A, B). This finding validated the observations of Su *et al.* (27), and also opened up a possible mechanistic avenue for the above observations.

DISCUSSION

In order to survive in the face of a robust host immune responses, pathogenic mycobacteria have developed a wide variety of adaptive strategies (9, 28). This study attempts to explain the involvement of the PE _PPE family proteins PPE25, PE18, and PPE26 in ESX-5-associated *M. tb* pathogenicity, by assessing their functional characteristics. Cell surface localization of members of this family (29, 30), prompted the hypothesis that they could influence pathogenesis by interacting with host receptors and dampening immune responses. Since there was a strong association between the expression patterns of these two genes in a dataset exhibiting global transcriptional responses of *M. tb* to inhibitors of metabolism (25, 31), it was hypothesised that these genes are operonic, a premise that we confirmed in our co-transcriptional analysis. This observation was further validated by performing growth dependent expression analyses of these genes in *M.tb* H37Rv, where the two genes were seen to be co-ordinately expressed in all growth phases from log to stationary. While our finding that PPE25 and PPE26 physically interact

was not surprising given the commonality of interaction between the products of co-ordinately expressed genes, based on experience working with PE-PPE clusters (32), we also expected to detect PPE25-PE18 and/or PPE26-PPE18 interactions in our assays, which we did not. Our discovery of PPE25 and PPE26 being the sole interacting pair therefore becomes even more significant considering the role of the ESX5-encoded type VII secretion system in *M. tb* pathogenesis. This also represents the second identification of PPE-PPE interaction, providing credence to our earlier finding of interaction between PPE50 and PPE51 (https://www.biorxiv.org/content/10.1101/2023.03.30.534876v1). In contrast to our results with PPE50 and PPE51, *M. smegmatis* strains expressing *PPE25*, *PPE26*, and *PE18* showed enhanced intra-macrophage survival compared to the control strain - with the increase in CFUs correlating with a decrease in *iNOS2* levels. Surprisingly, the recombinant strain expressing the entire operon did not show improved survival compared to controls in the THP-1 macrophage infection model, indicating a possible antagonistic role for the PPE25-PPE26 heterodimer in the independent CFU control function of the two proteins. *iNOS2* levels were significantly upregulated over the control levels in this scenario, possibly explaining the lack of CFU enhancement seen in the context of recombinants expressing the individual genes.

Because this cluster was found in the virulence-related *ESX-5* gene locus and the genes were upregulated under conditions of hypoxia and dormancy (15), we hypothesised that either protein might play a role in shifting the balance of cytokines in a way that helps let *M. tb* infection take hold and persist. In support of this premise, cytokine measurements following infection of THP-1 macrophages with recombinant strains expressing the cluster genes individually or as a whole, showed that all the cluster proteins can mediate the intra-macrophage lowering of IL-12p70 levels and an increase in IL-10 expression in macrophages. Consistent with the established TLR2 binding activity of PPE26 (27), THP-1 macrophages infected with recombinant strains *M. smegmatis* expressing *PPE26* & *PPE25-PE18-PPE26* showed enhanced P38 phosphorylation. It is highly likely that that the modulation of IL-10 and IL-12 by these proteins is mediated through the TLR2- P38 MAPK axis, a hypothesis that is currently being verified by experiments using inhibitors of this pathway.

It is known that signalling cascades downstream of TLR2 may result in expression level changes of pro- or anti-inflammatory cytokines, depending on the circumstances. PPE18, a member of the PE family, interacts with TLR2 to promote IL-10 induction (33). In contrast, PE_PGRS33 and lipoarabinomannan mediate signalling via TLR2-dependent pathways to promote the release of pro-inflammatory cytokines (34, 35). The mechanisms that determine whether a TLR2-triggered cascade will result in a pro-inflammatory or anti-inflammatory response are not well understood. Although it is known that *M. tb* may manipulate IL-10 in a way that increases its chances of survival (8, 9, 36), more work is needed to identify the effectors or processes involved in activating IL-10 production. Our findings contribute to the growing body of data suggesting that the PE/PPE family encodes numerous effectors involved in immunomodulation through IL-10 overexpression and IL-12 downregulation (9). Further studies will be required to validate our prediction of the *PPE25-PE18-PPE26* cluster contributing to survival of *M. tb via* controlling the expression of *IL-10*, *IL-12*, and *iNOS2*. For this, we propose to construct and examine the phenotypes of *M. tb H37Rv*Δ*PPE25*, Δ*PPE26*, and *ΔPPE25-PE-18-PPE26* strains in the THP-1 macrophage model and animal models of infection.

The findings presented here demonstrate that the *PPE25-PE18-PPE26* cluster may contribute to the establishment and maintenance of *M. tb* infection as a result of its immunomodulatory capacity (Fig. 5). Evidence from this research also suggests that the PPE proteins possess unique functions in their monomeric form, and may have additional, and possibly opposing functions when they hetero-dimerise with other PPE proteins.

Conflict of interest

The authors declare that there are no conflicts of interest.

Funding information

This work was supported by grant from the Council of Scientific and Industrial Research (MLP 0144)), Government of India (CSIR) (to T. R. R.). The funders had no role in study design, data collection and analysis, decision to publish, or preparation of the manuscript. R.P.M. was supported by a Senior Research

Fellowships from the Department of Biotechnology, Government of India (DBT), K. P. was supported by a fellowship from CSIR (MLP 0144), K. C. is supported by a Senior Research Fellowships from the CSIR.

Author contributions

T. R. R. designed the study. R. P. M., K. P., and K. C. performed the experiments. T. R. R. and R.P.M. analysed the data. T.R.R. and R. P. M. wrote the manuscript.

FIGURE LEGENDS

Figure 1: *PPE25*, *PE18*, and *PPE26* are co-transcribed, and the PPE25 and PPE26 gene products interact. A) The genomic organisation of the *PPE25-PE18-PPE26* region of the *M. tb* genome is shown schematically to highlight the positions of the gene (G) and junction (J) specific primers used in the experiment. (B) RT-PCR products amplified from the *PPE25-PE18-PPE26* cluster: lane 1: (25F+25R), lane 2: (25JF+18JR), lane 3: (18F+18F), lane 4: (18JF+26JR), lane 5: (26GF+26GR), lane 6: 100 bp DNA ladder, lanes 7-11: -RT controls for the respective primer pairs. (C) Real-time RT-PCR quantification of *PPE25*, *PE18*, *PPE26* and *PPE25-PE18-PPE26* transcripts as a function of *M. tb* H37Rv growth. Transcript levels are shown relative to the cognate gene's mRNA levels at 0.8 OD, which is given a value of 1. The error bars represent ± SEM (D) M-PFC analysis of pair-wise interaction between PPE25+PPE26, PPE25+PPE18, and PPE26+PPE18. The image depicts the growth pattern of *M. smegmatis* co-transformants on Middlebrook 7H11 agar plates with (+) or without (-) 20µg/ml trimethoprim (TRIM). The circled sample marks positivity for PPE25-PPE26 interaction. (E) Immunoblot of PPE25-PPE26 co-IP reactions from *M. smegmatis* expressing PPE26-c-myc and PPE25-6xHis. An anti-c-myc antibody was used to pull-down the complex, and the blot was probed with an anti-His antibody. The findings are based on at least two biological replicates

Figure 2: Phenotypes of recombinant *M. smegmatis* expressing*PPE25*, *PE18*, PPE26 and *PPE25-PE18-PPE26,* in THP-1 macrophages. (A) Post-infection CFU counts of recombinant strains of *M. smegmatis* expressing pMV261, *PPE25*, *PE18*, *PPE26* and *PPE25-PE18-PPE26* in THP-1 macrophages at 24 h, 48 h and 72 h. (B) input and post-infection (T_0) CFU counts of infecting bacilli (±SEM). (C) Real time RT-PCR quantitated *iNOS2* transcript levels in THP-1 macrophages infected with *M. smegmatis* expressing pMV261, *PPE25*, *PE18*, *PPE26* and *PPE25-PE18-PPE26*, 24 h, 48 h, and 72 h post-infection. The data is representative of two biological replicates. Error bars represent ± SEM. *p≤0.05, **p≤0.005, ***p ≤0.001. Error bars represent the mean ± SEM of two biological replicates.

Figure 4: Figure 3: Assessment of immunomodulatory potential (A) Transcript levels of *IL-10* in THP-1 macrophages infected with recombinant *M. smegmatis* strains expressing *PPE25*, *PE18*, *PPE26* and *PPE25-PE18-PPE26*, 24 h,48 h, and

72h post-infection. (B) Expression levels of the *IL-12* transcript in the same cells. Error bars represent ± SEM from two biological replicates. ***p<0.001, **p<0.005, * p<0.05.

Figure 4: Induction of TLR2 signalling. (A) Western blots depicting levels of total and Phospho-P38, and β-actin in lysates from THP-1 macrophages infected with recombinant strains of *M. smegmatis* expressing pMV261 (29) *PPE25* (25), *PE18* (18), *PPE26* (26), and the entire operon (25/18/26). The densitometric quantitation of this data is represented in (B).

Figure 5: Model illustrating the immunomodulatory functions of PE25 and PPE26 in the pathophysiology of *M. tb* MΦ - Macrophage

BIBLIOGRAPHY

1. Behar SM, Sassetti CM. 2014. Immunology: Fixing the odds against tuberculosis. Nature 511:39-40.
2. Bozzano F, Marras F, De Maria A. 2014. Immunology of tuberculosis. Mediterr J Hematol Infect Dis 6:e2014027.
3. Kincaid EZ, Wolf AJ, Desvignes L, Mahapatra S, Crick DC, Brennan PJ, Pavelka MS, Jr., Ernst JD. 2007. Codominance of TLR2-dependent and TLR2-independent modulation of MHC class II in Mycobacterium tuberculosis infection in vivo. J Immunol 179:3187-95.
4. Abdallah AM, Gey van Pittius NC, DiGiuseppe Champion PA, Cox J, Luirink J, Vandenbroucke-Grauls CM, Appelmelk BJ, Bitter W. 2007. Type VII secretion--mycobacteria show the way. Nat Rev Microbiol 5:883-91.
5. DiGiuseppe Champion PA, Cox JS. 2007. Protein secretion systems in Mycobacteria. Cell Microbiol 9:1376-84.
6. Sampson SL. 2011. Mycobacterial PE/PPE proteins at the host-pathogen interface. Clin Dev Immunol 2011:497203.
7. Akhter Y, Ehebauer MT, Mukhopadhyay S, and Hasnain SE. 2012. The PE/PPE multigene family codes for virulence factors and is a possible source of mycobacterial antigenic variation: perhaps more? Biochimie 94:110-6.
8. Mukhopadhyay S, Balaji KN. 2011. The PE and PPE proteins of *Mycobacterium tuberculosis*. Tuberculosis (Edinb) 91:441-7.
9. Tiwari BM, Kannan N, Vemu L, Raghunand TR. 2012. The Mycobacterium tuberculosis PE proteins Rv0285 and Rv1386 modulate innate immunity and mediate bacillary survival in macrophages. PLoS One 7:e51686.
10. Gey van Pittius NC, Sampson SL, Lee H, Kim Y, van Helden PD, Warren RM. 2006. Evolution and expansion of the *Mycobacterium tuberculosis* PE and PPE multigene families and their association with the duplication of the ESAT-6 (*esx*) gene cluster regions. BMC Evol Biol 6:95-.
11. Bottai D, Di Luca M, Majlessi L, Frigui W, Simeone R, Sayes F, Bitter W, Brennan MJ, Leclerc C, Batoni G, Campa M, Brosch R, Esin S. 2012. Disruption of the ESX-5 system of Mycobacterium tuberculosis causes loss of PPE protein secretion, reduction of cell wall integrity and strong attenuation. Mol Microbiol 83:1195-209.

12. Sayes F, Sun L, Di Luca M, Simeone R, Degaiffier N, Fiette L, Esin S, Brosch R, Bottai D, Leclerc C, Majlessi L. 2012. Strong immunogenicity and cross-reactivity of Mycobacterium tuberculosis ESX-5 type VII secretion: encoded PE-PPE proteins predicts vaccine potential. Cell Host Microbe 11:352-63.
13. McNamara M, Danelishvili L, Bermudez LE. 2012. The Mycobacterium avium ESX-5 PPE protein, PPE25-MAV, interacts with an ESAT-6 family Protein, MAV_2921, and localizes to the bacterial surface. Microb Pathog 52:227-38.
14. Wu M, Li M, Yue Y, Xu W. 2016. DNA vaccine with discontinuous T-cell epitope insertions into HSP65 scaffold as a potential means to improve immunogenicity of multi-epitope Mycobacterium tuberculosis vaccine. Microbiol Immunol 60:634-45.
15. Majumdar SD, Vashist A, Dhingra S, Gupta R, Singh A, Challu VK, Ramanathan VD, Kumar P, Tyagi JS. 2012. Appropriate DevR (DosR)-mediated signaling determines transcriptional response, hypoxic viability and virulence of Mycobacterium tuberculosis. PLoS One 7:e35847.
16. Voskuil MI, Schnappinger D, Rutherford R, Liu Y, Schoolnik GK. 2004. Regulation of the *Mycobacterium tuberculosis* PE/PPE genes. Tuberculosis (Edinb) 84:256-62.
17. Sambrook J, Fritsch EF, Maniatis T. 1989. Molecular Cloning: A Laboratory Manual, 2nd edition. Cold Spring Harbor Laboratory Press, Cold Spring Harbor, New York.
18. Hofmann K, and W. Stoffel 1993. TMbasc—a database of membrane spanning protein segments. Biol Chem Hoppe-Seyler 374:166.
19. Kyte J, Doolittle RF. 1982. A simple method for displaying the hydropathic character of a protein. J Mol Biol 157:105-32.
20. Spratt JM, Ryan AA, Britton WJ, Triccas JA. 2005. Epitope-tagging vectors for the expression and detection of recombinant proteins in mycobacteria. Plasmid 53:269-73.
21. Cascioferro A, Delogu G, Colone M, Sali M, Stringaro A, Arancia G, Fadda G, Palu G, Manganelli R. 2007. PE is a functional domain responsible for protein translocation and localization on mycobacterial cell wall. Mol Microbiol 66:1536-47.
22. Stover CK, Bansal GP, Hanson MS, Burlein JE, Palaszynski SR, Young JF, Koenig S, Young DB, Sadziene A, Barbour AG. 1993. Protective immunity

elicited by recombinant bacille Calmette-Guerin (BCG) expressing outer surface protein A (OspA) lipoprotein: a candidate Lyme disease vaccine. J Exp Med 178:197-209.

23. Stover CK, de la Cruz VF, Fuerst TR, Burlein JE, Benson LA, Bennett LT, Bansal GP, Young JF, Lee MH, Hatfull GF, et al. 1991. New use of BCG for recombinant vaccines. Nature 351:456-60.

24. Singh A, Mai D, Kumar A, Steyn AJ. 2006. Dissecting virulence pathways of *Mycobacterium tuberculosis* through protein-protein association. Proc Natl Acad Sci U S A 103:11346-51.

25. Mohareer K, Tundup S, Hasnain SE. 2011. Transcriptional regulation of Mycobacterium tuberculosis PE/PPE genes: a molecular switch to virulence? J Mol Microbiol Biotechnol 21:97-109.

26. Flynn JL, Chan J. 2001. Immunology of tuberculosis. Annu Rev Immunol 19:93-129.

27. Su H, Kong C, Zhu L, Huang Q, Luo L, Wang H, Xu Y. 2015. PPE26 induces TLR2-dependent activation of macrophages and drives Th1-type T-cell immunity by triggering the cross-talk of multiple pathways involved in the host response. Oncotarget 6:38517-37.

28. Ganguly N, Siddiqui I, Sharma P. 2008. Role of *M. tuberculosis* RD-1 region encoded secretory proteins in protective response and virulence. Tuberculosis (Edinb) 88:510-7.

29. Banu S, Honoré N, Saint-Joanis B, Philpot D, Prévost M, Cole ST. 2002. Are the PE-PGRS proteins of *Mycobacterium tuberculosis* variable surface antigens? Molecular Microbiology 44: 9–19.

30. Demangel C, Brodin P, Cockle PJ, Brosch R, Majlessi L, Leclerc C, Cole ST. 2004. Cell envelope protein PPE68 contributes to Mycobacterium tuberculosis RD1 immunogenicity independently of a 10-kilodalton culture filtrate protein and ESAT-6. Infect Immun 72:2170-6.

31. Boshoff HI, Myers TG, Copp BR, McNeil MR, Wilson MA, Barry CE, 3rd. 2004. The transcriptional responses of *Mycobacterium tuberculosis* to inhibitors of metabolism: novel insights into drug mechanisms of action. J Biol Chem 279:40174-84.

32. Tiwari B, Soory A, Raghunand TR. 2014. An immunomodulatory role for the Mycobacterium tuberculosis region of difference 1 locus proteins PE35 (Rv3872) and PPE68 (Rv3873). FEBS J 281:1556-70.

33. Nair S, Ramaswamy PA, Ghosh S, Joshi DC, Pathak N, Siddiqui I, Sharma P, Hasnain SE, Mande SC, Mukhopadhyay S. 2009. The PPE18 of Mycobacterium tuberculosis interacts with TLR2 and activates IL-10 induction in macrophage. J Immunol 183:6269-81.

34. Underhill DM, Ozinsky A, Smith KD, Aderem A. 1999. Toll-like receptor-2 mediates mycobacteria-induced proinflammatory signaling in macrophages. Proc Natl Acad Sci U S A 96:14459-63.

35. Basu S, Pathak SK, Banerjee A, Pathak S, Bhattacharyya A, Yang Z, Talarico S, Kundu M, Basu J. 2007. Execution of macrophage apoptosis by PE_PGRS33 of *Mycobacterium tuberculosis* is mediated by Toll-like receptor 2-dependent release of tumor necrosis factor-alpha. J Biol Chem 282:1039-50.

36. Saraiva M, O'Garra A. 2010. The regulation of IL-10 production by immune cells. Nat Rev Immunol 10:170-81.

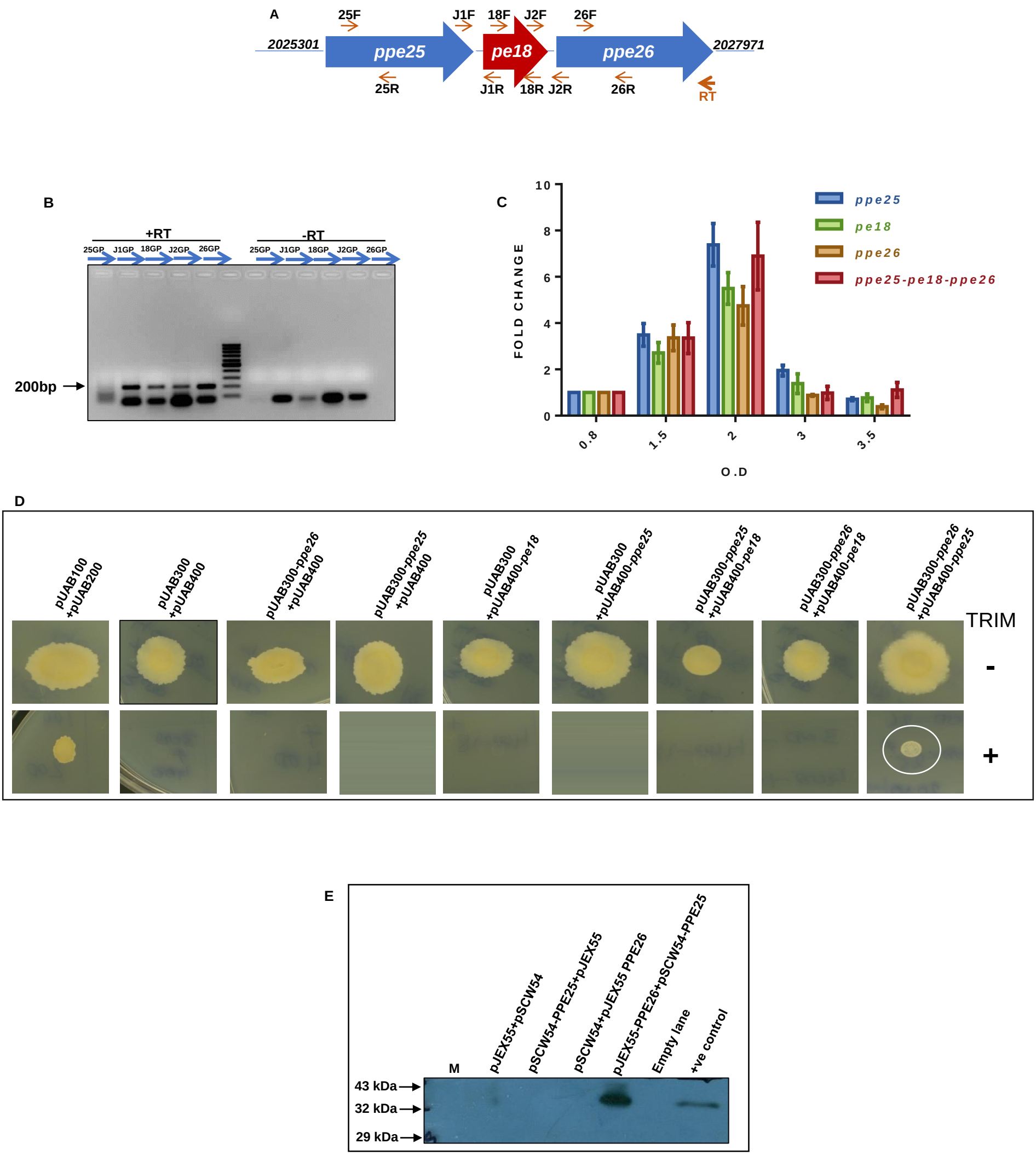
A
25F
J1F
18F
J2F
26F
2025301
ppe25
pe18
ppe26
2027971
25R
J1R
18R
J2R
26R
RT
B
+RT
-RT
25GP
J1GP
18GP
J2GP
26GP
200bp
C
FOLD CHANGE
O.D
0.8
1.5
2
3
3.5
ppe25
pe18
ppe26
ppe25-pe18-ppe26
D
pUAB100 +pUAB200
pUAB300 +pUAB400
pUAB300-ppe26 +pUAB400
pUAB300-ppe25 +pUAB400
pUAB300 +pUAB400-pe18
pUAB300 +pUAB400-ppe25
pUAB300-ppe25 +pUAB400-pe18
pUAB300-ppe26 +pUAB400-pe18
pUAB300-ppe26 +pUAB400-ppe25
TRIM
-
+
E
M
pJEX55+pSCW54
pSCW54-PPE25+pJEX55
pSCW54+pJEX55 PPE26
pJEX55-PPE26+pSCW54-PPE25
Empty lane
+ve control
43 kDa
32 kDa
29 kDa

Figure1

A

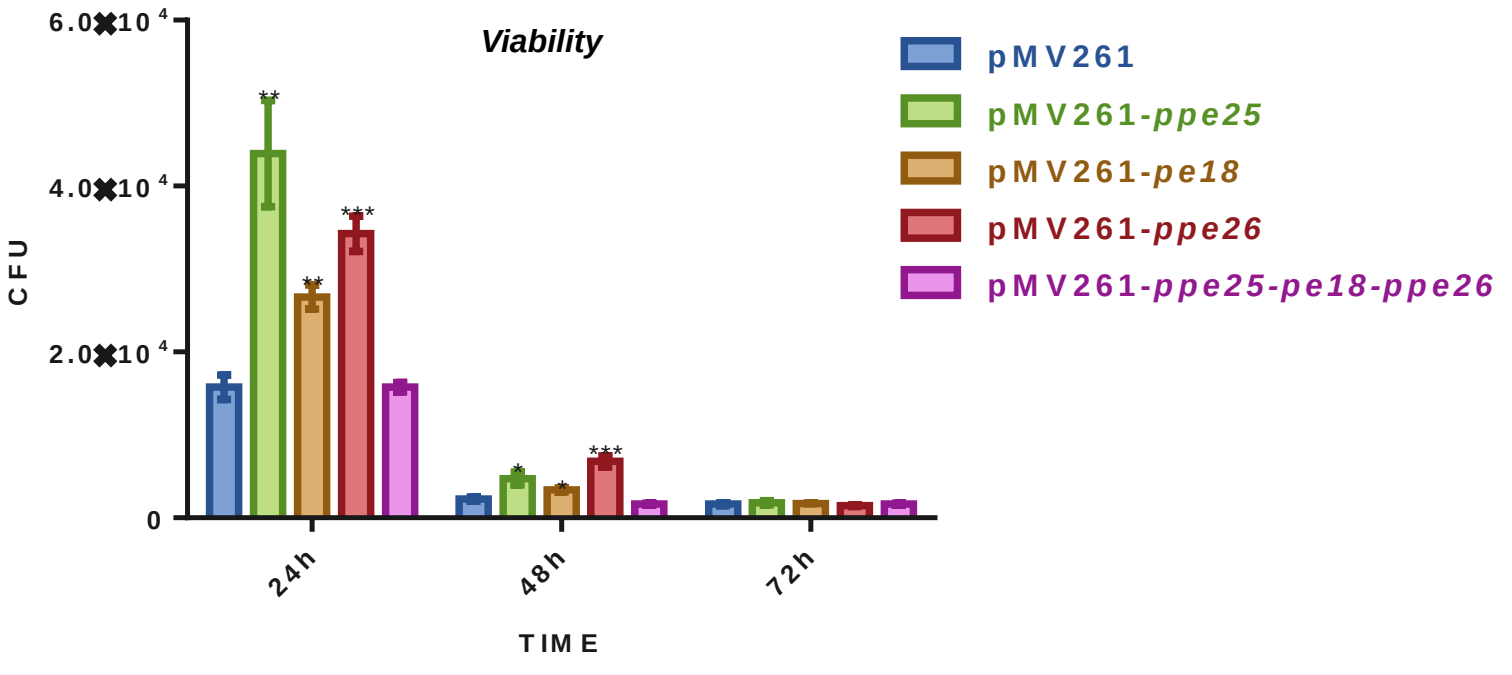

B

	pMV261	pMV261- *ppe25*	pMV261- *pe18*	pMV261-*ppe26*	pMV261-*ppe25-pe18-ppe26*
Input	3.03 ± .022x 10^8	3.05 ± 0.27x 10^8	3.16 ± 0.8x 10^8	2.90 ± .10x 10^8	3.31 ± 19x 10^5
T_0	90.92 ± 34x 10^5	90.02 ± 28x 10^5	99.92 ± 39x 10^5	84.67 ± 25x 10^5	87.05 ± 22x 10^5

C

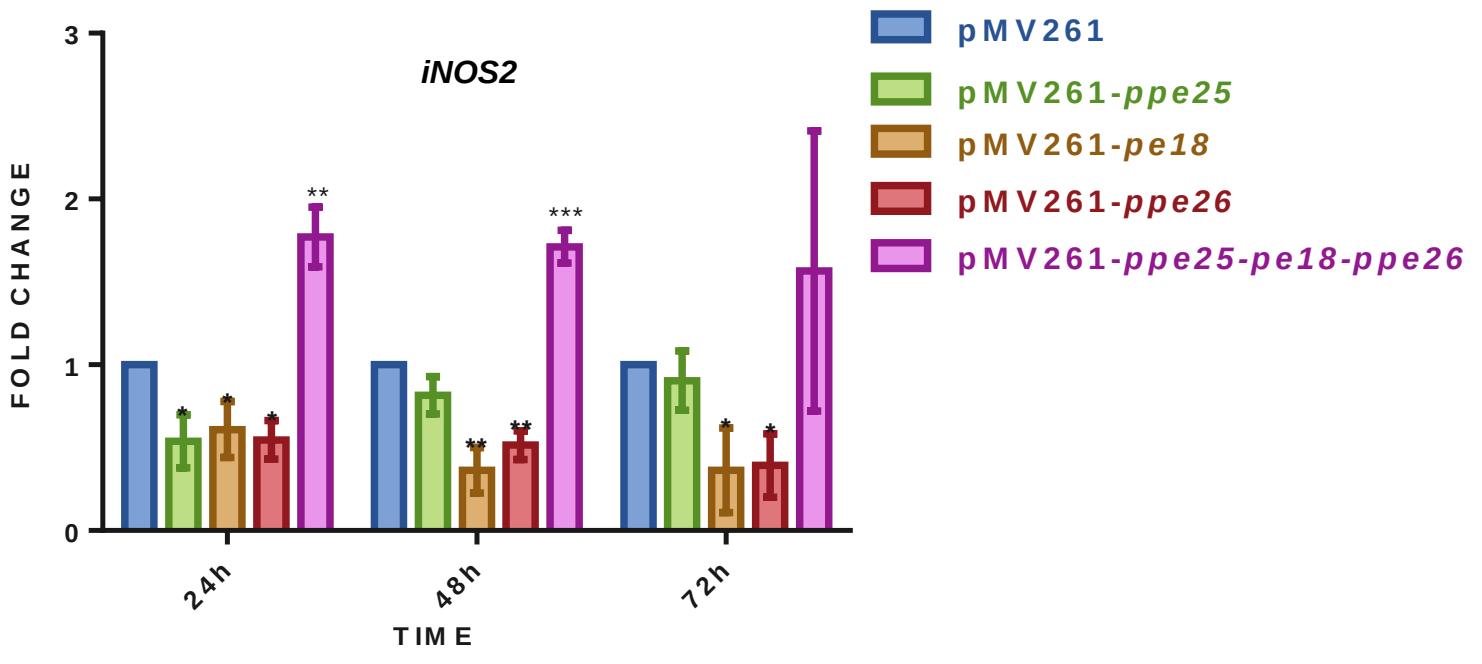

Figure 2

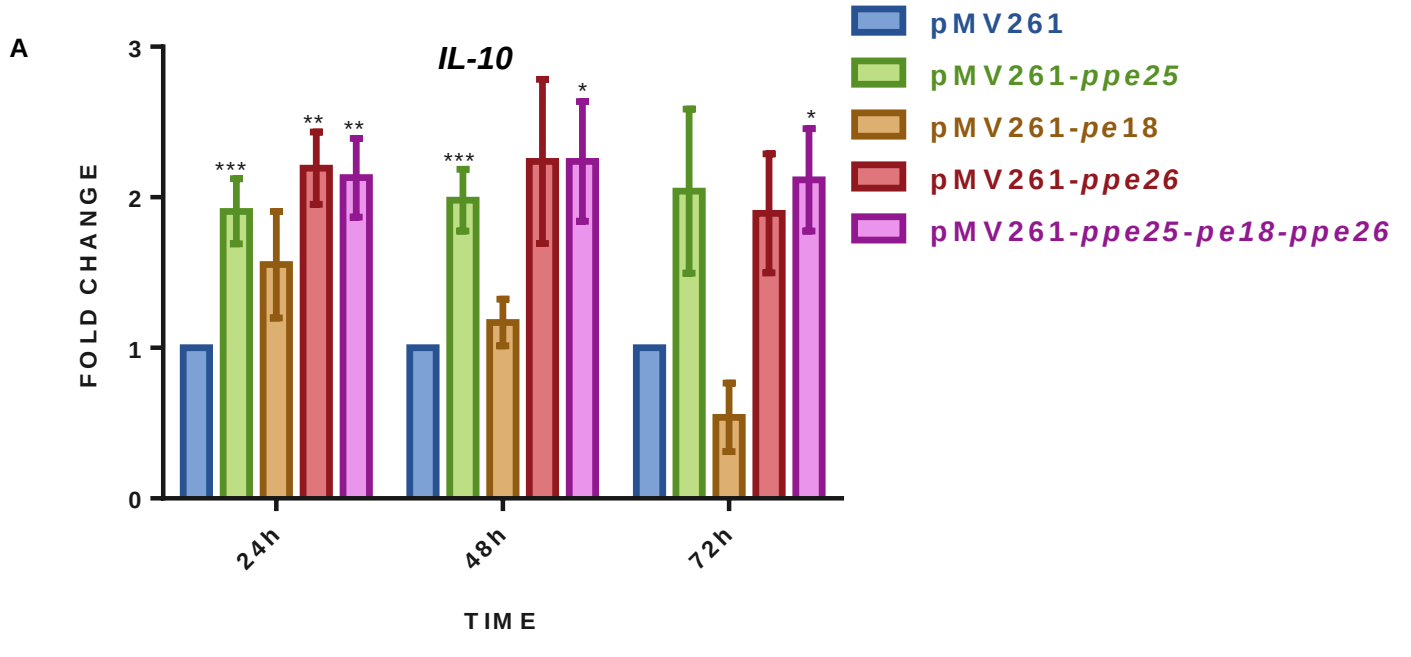
A
IL-10
FOLD CHANGE
3
2
1
0
***
**
**
***
*
*
24h
48h
72h
TIME
pMV261
pMV261-ppe25
pMV261-pe18
pMV261-ppe26
pMV261-ppe25-pe18-ppe26

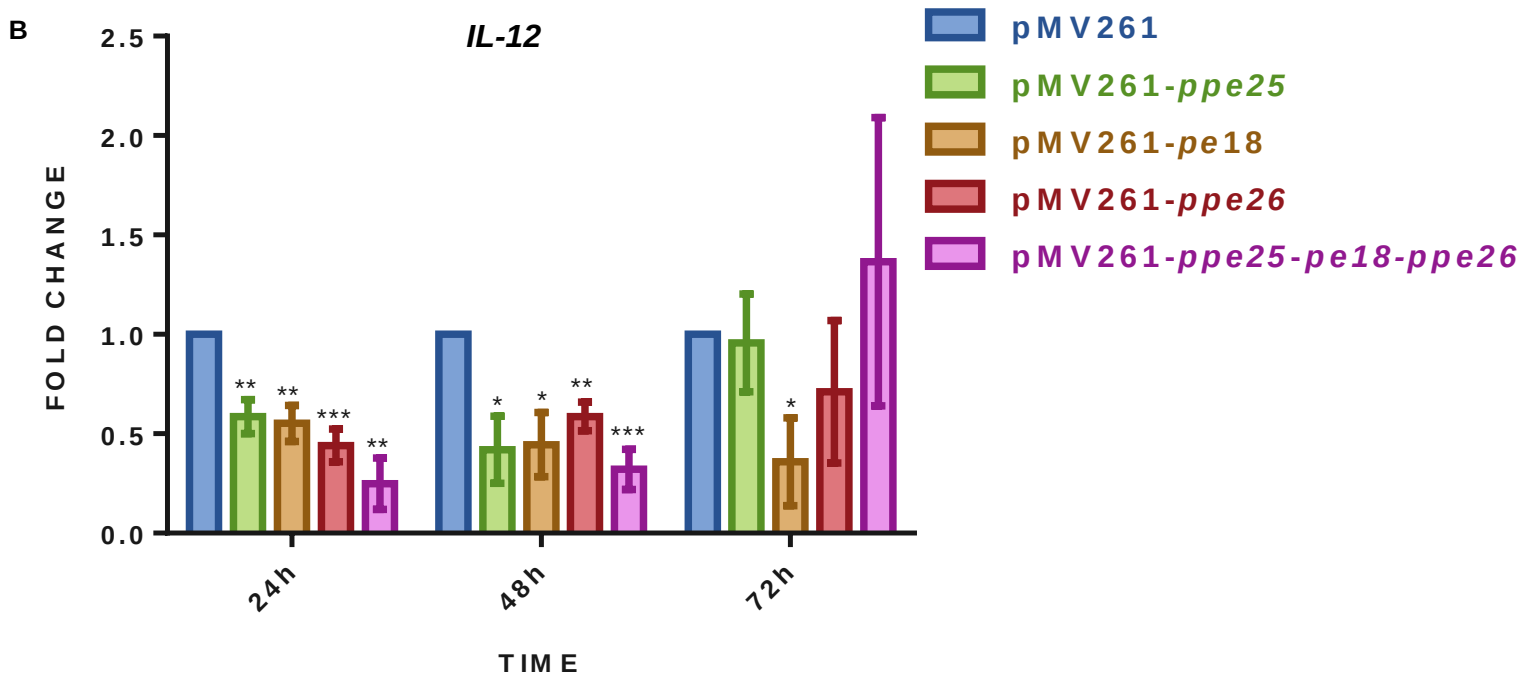
B
IL-12
FOLD CHANGE
2.5
2.0
1.5
1.0
0.5
0.0
**
**
***
**
*
*
**
***
*
24h
48h
72h
TIME
pMV261
pMV261-ppe25
pMV261-pe18
pMV261-ppe26
pMV261-ppe25-pe18-ppe26

Figure 3

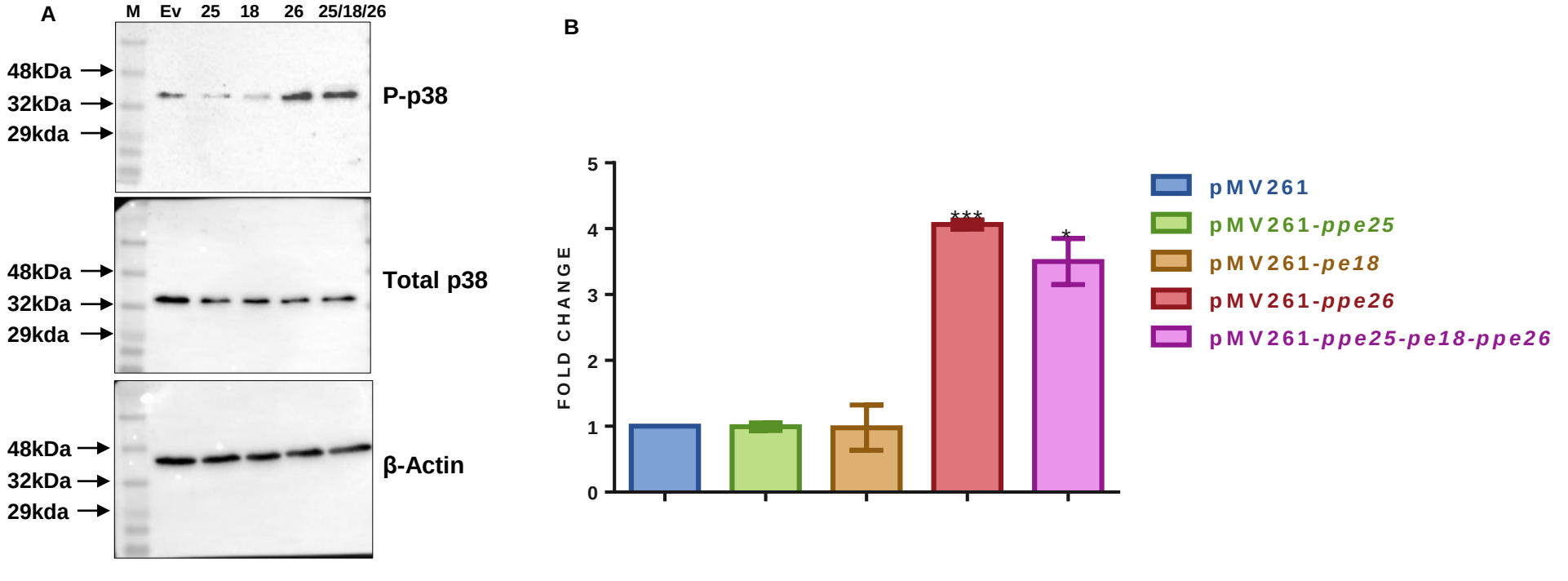
A
M
Ev
25
18
26
25/18/26
48kDa
32kDa
29kda
P-p38
Total p38
β-Actin
B
FOLD CHANGE
0
1
2
3
4
5
***
*
pMV261
pMV261-ppe25
pMV261-pe18
pMV261-ppe26
pMV261-ppe25-pe18-ppe26

Figure 4

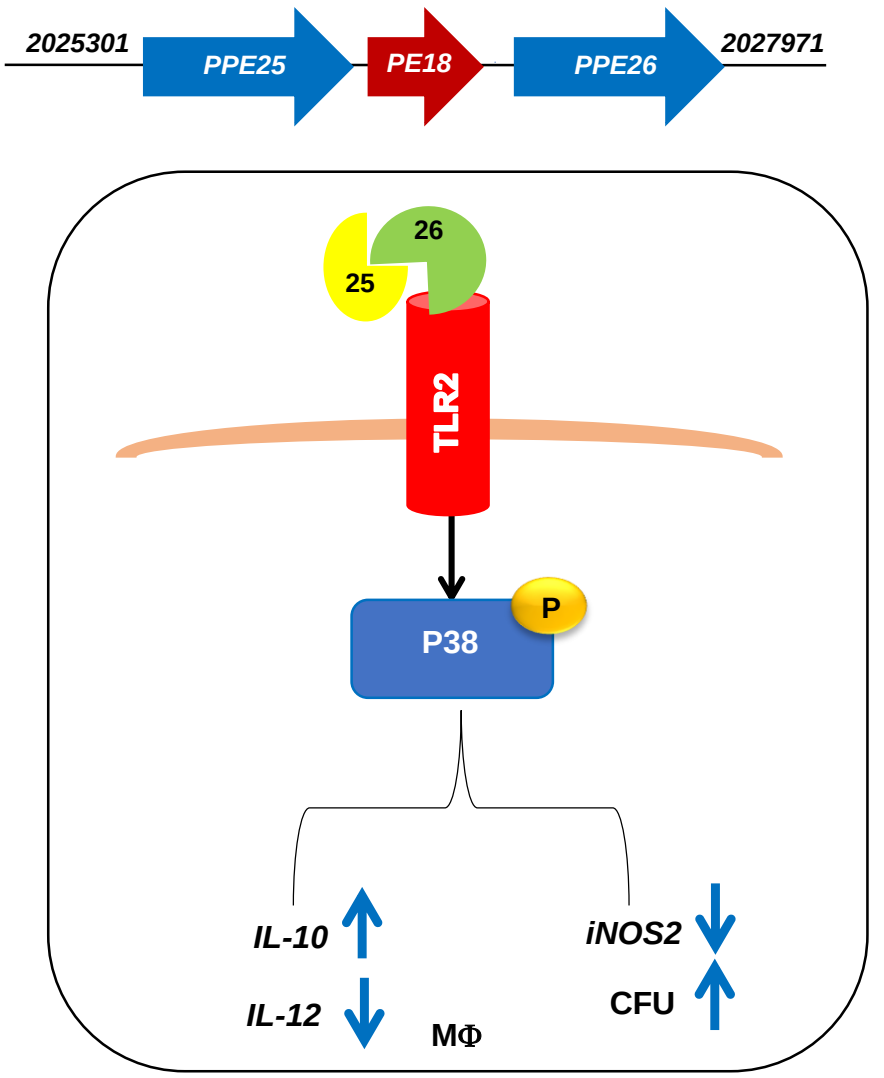
2025301
PPE25
PE18
PPE26
2027971
26
25
TLR2
P
P38
IL-10
IL-12
iNOS2
CFU
MΦ

Figure 5